

## Projected changes of rainfall event characteristics for the Czech Republic

Vojtěch Svoboda<sup>1</sup>, Martin Hanel<sup>1, 2\*</sup>, Petr Máca<sup>1</sup>, Jan Kyselý<sup>1, 3</sup>

<sup>1</sup> Faculty of Environmental Sciences, Czech University of Life Sciences Prague, Kamýcká 129, 165 21 Prague 6–Suchbát, Czech Republic.

<sup>2</sup> Technical University of Liberec, Studentská 1402/2, 461 17 Liberec 1, Czech Republic.

<sup>3</sup> Institute of Atmospheric Physics, Czech Academy of Sciences, Boční II 1401, 141 31 Prague 4–Spořilov, Czech Republic.

\* Corresponding author. Tel.: +420 22438 3834. E-mail: hanel@fzp.czu.cz

**Abstract:** Projected changes of warm season (May–September) rainfall events in an ensemble of 30 regional climate model (RCM) simulations are assessed for the Czech Republic. Individual rainfall events are identified using the concept of minimum inter-event time and only heavy events are considered. The changes of rainfall event characteristics are evaluated between the control (1981–2000) and two scenario (2020–2049 and 2070–2099) periods. Despite a consistent decrease in the number of heavy rainfall events, there is a large uncertainty in projected changes in seasonal precipitation total due to heavy events. Most considered characteristics (rainfall event depth, mean rainfall rate, maximum 60-min rainfall intensity and indicators of rainfall event erosivity) are projected to increase and larger increases appear for more extreme values. Only rainfall event duration slightly decreases in the more distant scenario period according to the RCM simulations. As a consequence, the number of less extreme heavy rainfall events as well as the number of long events decreases in majority of the RCM simulations. Changes in most event characteristics (and especially in characteristics related to the rainfall intensity) depend on changes in radiative forcing and temperature for the future periods. Only changes in the number of events and seasonal total due to heavy events depend significantly on altitude.

**Keywords:** Rainfall event; Hourly rainfall; Regional climate model; Climate change.

### INTRODUCTION

Potential changes in characteristics of precipitation events such as event depth, duration or intensity due to climate change are of significant societal concern, especially after evidence of increasing daily extreme rainfall intensity has strengthened (Alexander et al., 2006; Trenberth, 2011; Westra et al., 2014). Central Europe has been affected by several major flood events in the recent decades (e.g. Kundzewicz et al., 2005; Kundzewicz, 2012). These floods resulted either from heavy multi-day rainfall events affecting large areas (e.g. Blöschl et al., 2013) or from localized extreme sub-daily events (e.g. Marchi et al., 2010). Especially short duration extreme events might intensify more in future climate due to dynamical feedbacks (Berg and Haerter, 2013; Lenderink and van Meijgaard, 2008; Millán, 2014).

A comprehensive overview of the assessment studies on trends in precipitation extremes and floods across Europe is given by Madsen et al. (2014). Over the Czech Republic, Kyselý (2009) evaluated seasonal trends in heavy precipitation on daily basis for 1961–2005. In winter, spatially coherent increases were reported mainly in the western part of the country. The trends were spatially less uniform in summer, but increasing tendency in heavy precipitation prevailed. Decreases were observed in spring, while the least spatially coherent and insignificant trends were found in autumn.

Only a limited number of studies analysed sub-daily rainfall extremes (e.g. Beck et al., 2015; Jakob et al., 2011; Lenderink et al., 2011). For the Czech Republic, Hanel et al. (2016) analysed trends in characteristics of sub-daily heavy precipitation (at various aggregation levels from 30-min to 1-day) considering 17 stations and 51 years (May–September periods for 1961–2011). Observed trends in indices of heavy precipitation (seasonal maxima; rain intensity index; fractions of precipitation due to very wet days) were significant and positive for many of the stations (an average increase of 2–9% per decade for all examined characteristics).

Recently, Rulfová and Kyselý (2014) analysed characteristics of convective and stratiform precipitation separately at 11 stations for 1982–2010. They found that spatially averaged trends in convective precipitation were positive for rainfall totals and the number of wet days in spring, summer and autumn, and tended to be more pronounced at lowland stations. The trends in extreme convective precipitation (maximum seasonal 6-hour and 1-day totals) were spatially more variable and often insignificant, but slight increase prevailed as well. The observed increase in total precipitation in spring and summer was mainly due to an increase in convective precipitation (Rulfová and Kyselý, 2014).

Events with high rainfall depths and durations of a few hours are most often associated with convective storms (Hand et al., 2004; Westra et al., 2014). Rulfová and Kyselý (2013) reported that the convective precipitation represents about 50% of the total precipitation in summer for the Czech Republic, and heavy rainfall events contribute significantly to precipitation in warm season.

Despite the relevance to urban hydrology or soil erosion assessment, only a few studies dealt with characteristics of individual rainfall events derived from observed rainfall data. Fiener et al. (2013), for instance, found significant trends in annual rainfall erosivity in a long record (1937–2007) of 5-min precipitation data for 10 stations in Germany. Hanel et al. (2016) assessed erosive rainfall events for the 1961–2011 period in the Czech Republic and found significant increasing trends in event rainfall rate and significant decreasing trends in event duration.

To obtain estimates of possible future changes in precipitation at a regional or local scale, regional climate models (RCMs) are widely used. Studies on precipitation extremes in ensembles of RCM simulations over the area of the Czech Republic (Hanel and Buishand, 2012; Kyselý and Beranová, 2009; Kyselý et al., 2011) reported increases in summer and winter 1-day precipitation extremes for the late 21<sup>st</sup> century (increases in the 50-year quantile ~ 16–26%). Comparable

future changes in daily summer precipitation extremes were indicated also for many other locations in Europe (e.g. Frei et al., 2006; Hanel and Buishand, 2011; Madsen et al., 2014).

While the simulated changes in precipitation extremes at daily and multi-day time scales are explored relatively well, only few studies considered changes at sub-daily time scales. For instance, based on RCM simulations and climate analogues, Arnbjerg-Nielsen (2012) estimated an increase in design sub-daily precipitation intensities in Denmark (up to 50% for hourly precipitation maxima and 100-year return period within the next 100 years). The projected increase in intensities tended to be larger with shorter durations and higher return periods. Hanel and Buishand (2010) analysed changes in hourly and daily summer precipitation extremes over the Netherlands using a statistical model. The estimated changes in annual daily maxima were relatively small ( $\approx 20\%$  for return periods larger than 5 years). A similar value was found also for hourly extremes, when the statistical model was constrained to allow for changes only in the first two moments of the distribution; however, an unconstrained model revealed  $\approx 45\text{--}60\%$  increase in 50 to 200-year precipitation maxima indicating large uncertainty in projected changes of high quantiles. Large increases in simulated heavy summer precipitation were also mentioned by Lenderink and van Meijgaard (2008) for the Netherlands and Kendon et al. (2014) for the UK, while Knote et al. (2010) and Pan et al. (2011) reported decreases for Germany and Western U.S., respectively.

The majority of available RCM simulations (having spatial resolution coarser than 10 km) relies on convection parameterization schemes, which are sources of significant uncertainties and errors (Brockhaus et al., 2008; Hohenegger et al., 2008; Kendon et al., 2012) especially for sub-daily precipitation (Westra et al., 2014). The deficiencies in simulating convective precipitation may significantly affect the estimated changes in rainfall extremes (Kendon et al., 2014).

The purpose of this paper is to analyse changes of heavy rainfall event characteristics between the control (1981–2010) and two scenario periods (2020–2049 and 2070–2099) as projected by an ensemble of RCM simulations with hourly data conducted within the ENSEMBLES (van der Linden and Mitchell, 2009) and EURO-CORDEX (Jacob et al., 2014) projects.

The paper is organized as follows. The study area and RCM data are described in following section. Section Methods provides definition of heavy rainfall events, considered event characteristics and approaches for the assessment of changes in RCM-simulated rainfall events. The changes in RCM-simulated

heavy rainfall events are given in the Results section. The paper is closed by Discussion and Summary.

## STUDY AREA AND THE RCM SIMULATIONS

Projected changes in RCM-simulated rainfall event characteristics are analysed for the Czech Republic (78800 km<sup>2</sup>) located in Central Europe (Fig. 1a). Approximately two-thirds of the area are situated in altitudes below 500 m, while several mountain ranges on the borders exceed 1200 m in elevation (maximum is about 1600 m in the north; Fig. 1b). Average annual precipitation totals for the 1961–2000 period vary from about 420 mm in the central-western part of the country up to more than 1200 mm in the mountains. Mean annual precipitation for the Czech Republic is about 670 mm and the wettest months at most stations are June and July (Tolasz, 2007). Almost two-thirds of the annual precipitation falls in the summer half of the year. During the summer half-year (April–September) the rainfall events usually have shorter durations and larger intensities, while during the winter half-year (October–March) the rainfall events are mainly characterized by lower intensities and longer durations, and are connected to low pressure and frontal systems (Tolasz, 2007).

The examined ensemble of 30 RCM simulations is described in Table 1. Six RCMs are driven by 14 global climate models (GCMs) forced by scenarios SRES A1B (Nakicenovic and Swart, 2000), RCP2.6, RCP4.5 or RCP8.5 (van Vuuren et al., 2011). The RCMs outputs are available on a rotated latitude-longitude grid with a horizontal resolution ranging from 12.5 to 50 km. Only the CLM simulation is on a regular grid. From each RCM simulation only grid boxes covering the area of the Czech Republic (i.e. 52–607 grid boxes for different RCMs) were selected (see Fig. 1b).

The HIRHAM5, HadRM3 and RACMO2 simulations were conducted within the ENSEMBLES project (van der Linden and Mitchell, 2009), while the RCA4 and RACMO22E simulations within the EURO-CORDEX project (Jacob et al., 2014). Two of the HadRM3 simulations are driven by the GCM version with perturbed physics parameterization (Collins et al., 2006). HadRM3Q0 is an unperturbed model run, HadRM3Q3 is a version with low sensitivity to external forcing, and HadRM3Q16 includes perturbations resulting in high sensitivity to external forcing. The perturbations in the HadRM3 RCM correspond to those in the HadCM3 GCM.

Projected changes were analysed between the control period (1981–2000) and two scenario periods (2020–2049 and 2070–2099).

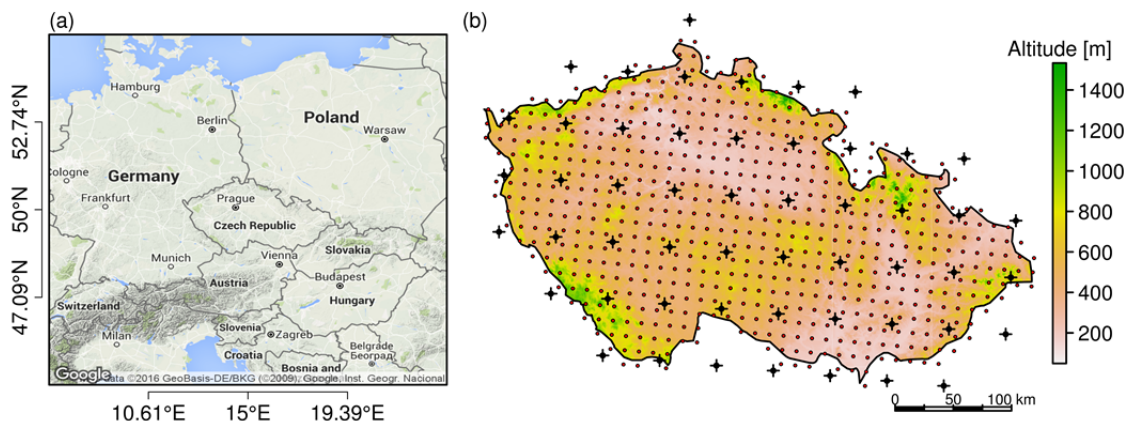


**Fig. 1.** (a) Location of the Czech Republic in Central Europe. (b) Centres of grid boxes covering the Czech Republic for RCM simulations with 50 km (black dots, 52 grid boxes) and 12.5 km spatial resolution (small red dots, 607 grid boxes).

**Table 1.** Overview of the RCM simulations.

| RCM Acronym  | Driven by GCM   | Forcing                | Horizontal resolution | Grid boxes |
|--|-----------------|------------------------|-----------------------|------------|
| <b>CLM 2.4.11</b> (Böhm et al. 2006; Lautenschlager et al. 2009a, b) – Max Planck Institute for Meteorology (MPI), Germany |                 |                        |                       |            |
| CLM  | ECHAM5/MPIOM    | SRES A1B               | 22 km (0.2°)          | 301        |
| <b>HadRM3.0</b> (Collins et al. 2011) – Met Office Hadley Centre (MOHC), UK  |                 |                        |                       |            |
| HadRM3Q0_HadCM3  | HadCM3Q0        | SRES A1B               | 25 km (0.22°)         | 173        |
| HadRM3Q3_HadCM3  | HadCM3Q3        |                        |                       |            |
| HadRM3Q16_HadCM3   | HadCM3Q16       |                        |                       |            |
| <b>HIRHAM5</b> (Christensen et al. 2007) – Danish Meteorological Institute (DMI)   |                 |                        |                       |            |
| H5_ARPEGE  | ARPEGE          | SRES A1B               | 25 km (0.22°)         | 173        |
| H5_BCM   | BCM             |                        |                       |            |
| H5_ECHAM5  | ECHAM5-r3       |                        |                       |            |
| <b>RACMO2.1</b> (van Meijgaard et al. 2008) – Royal Netherlands Meteorological Institute (KNMI)                            |                 |                        |                       |            |
| RACMO2_ECHAM5  | ECHAM5-r3       | SRES A1B               | 25 km (0.22°)         | 173        |
| RACMO2_MIROC   | MIROC3.2        |                        |                       |            |
| <b>RACMO22E</b> (van Meijgaard et al. 2012) – Royal Netherlands Meteorological Institute (KNMI)                            |                 |                        |                       |            |
| RACMO22E   | ICHEC-EC-EARTH  | RCP4.5, RCP8.5         | 12.5 km (0.11°)       | 607        |
| <b>RCA4.0</b> (Kupiainen et al. 2011; Samuelsson et al. 2011) – Swedish Meteorological and Hydrological Institute (SMHI)   |                 |                        |                       |            |
| RCA4_CanESM2   | CCCma-CanESM2   | RCP4.5, RCP8.5         | 50 km (0.44°)         | 52         |
| RCA4_CM5A-MR   | IPSL-CM5A-MR    | RCP4.5, RCP8.5         |                       |            |
| RCA4_CNRM-CM5  | CNRM-CM5        | RCP4.5, RCP8.5         |                       |            |
| RCA4_EC-EARTH  | ICHEC-EC-EARTH  | RCP2.6, RCP4.5, RCP8.5 |                       |            |
| RCA4_ESM2M   | NOAA-GFDL-ESM2M | RCP4.5, RCP8.5         |                       |            |
| RCA4_ESM-LR  | MPI-ESM-LR      | RCP4.5, RCP8.5         |                       |            |
| RCA4_HadGEM2-ES  | MOHC-HadGEM2-ES | RCP4.5, RCP8.5         |                       |            |
| RCA4_MIROC5  | MIROC5          | RCP4.5, RCP8.5         |                       |            |
| RCA4_NorESM1-M   | NCC-NorESM1-M   | RCP4.5, RCP8.5         |                       |            |

## METHODS

This section provides the definition of rainfall events and considered event characteristics. Methods for the analysis of changes in rainfall events are presented at the end of the section.

### Rainfall event definition

Rainfall events were defined using the minimum inter-event time (MIT) approach (e.g. Dunkerley, 2008). Six hour MIT was used for the derivation of rainfall events in all RCM simulations. This value is used most frequently for the identification of individual events in observed data (Dunkerley, 2008) and is typical also in rainfall erosion studies (e.g. Wischmeier and Smith, 1978). Please note, however, that the estimated optimal MIT for observed data over the Czech Republic is longer (Hanel and Máca, 2014). This holds true also for most of the RCM simulations for the Czech Republic in 1981–2000 (not shown).

In addition to 6-hour MIT a wet-hour threshold of 0.1 mm was considered in order to account for drizzling effect in the evaluation of RCM simulations (Kjellström et al., 2010). The same value was used also in previous studies (e.g. Kendon et al., 2014; Willems and Vrac, 2011). We further focused on 15% of rainfall events with the largest event depth during the warm season (May–September), which are referred to as heavy rainfall events in the rest of the paper. Note that for observed data this means that the threshold defining heavy rainfall events roughly corresponds to 12.7 mm, which is the minimum event

depth of a rainfall event to be considered erosive according to the Universal Soil Loss Equation methodology (Wischmeier and Smith, 1978).

### Rainfall event characteristics

We focused on projected future changes of the following rainfall event characteristics:

- rainfall event depth  $D$  [mm],
- rainfall event duration  $T$  [h],
- event mean rainfall rate  $RR$  [ $\text{mm}\cdot\text{h}^{-1}$ ]:

$$RR = \frac{D}{T} \quad (1)$$

- maximum 60-min rainfall intensity during an event  $I60$  [ $\text{mm}\cdot\text{h}^{-1}$ ].

In addition, the following indicators of erosive potential of a rainfall event were considered as well:

- event rainfall energy  $E$  [ $\text{MJ}\cdot\text{ha}^{-1}$ ]; Brown and Foster (1987):

$$E = \sum_{t=1}^T 0.29d_t[1 - 0.72\exp(-0.05d_t)] \quad (2)$$

where  $d_t$  is a rainfall volume during hour  $t$ .

- event rainfall erosivity index  $EI60$  [ $\text{MJ}\cdot\text{mm}\cdot\text{ha}^{-1}\cdot\text{h}^{-1}$ ]:

$$EI60 = E \cdot I60 \quad (3)$$

Finally, we analysed also projected changes in seasonal (May–September) characteristics:

- the number of heavy rainfall events per season  $Ne$  [–] and
- seasonal total due to heavy rainfall events  $TOT$  [mm].

### Assessment of projected changes of rainfall event characteristics

The changes of rainfall (event/seasonal) characteristics over two scenario periods: 2020–2049 (SCE1) and 2070–2099 (SCE2) with respect to the control period 1981–2000 were assessed in the RCM simulations for the Czech Republic as follows:

1) Rainfall events were determined for each grid box across the study area and all periods. Characteristics of rainfall events were calculated.

2) We evaluated changes in the RCM simulations between the scenario and control periods for:

- a) mean rainfall (event/seasonal) characteristics for each grid box over the study area (further denoted  $rts_m$ );
- b)  $p^{\text{th}}$  quantiles of the distribution of rainfall event characteristics for each grid box for cumulative probabilities  $p = 0.05, 0.1, \dots, 0.95$  (further referred to as quantile changes  $rts_p$ );
- c) areal average annual frequencies for corresponding bins of the histograms of rainfall event characteristics (further denoted as histogram changes  $rts_f$ ).

3) Because atmospheric temperature may influence the intensity of rainfall extremes (e.g. Utsumi et al., 2011; Westra et al., 2013), we analysed also relations of simulated rainfall event characteristics to changes in daily mean temperature ( $T2M$  [°C]) and radiative forcing ( $RFO$  [ $W \cdot m^{-2}$ ]). Radiative forcing as given by Houghton et al. (2001) for the SRES A1B emission scenario and Meinshausen et al. (2011) for the RCP scenarios was considered. Changes of radiative forcing and daily temperature for the scenario periods were calculated in the same way as  $rts_m$  for other (event/seasonal) characteristics. Then all  $rts_m$  were averaged over the study area (i.e. one  $rts_m$  value for each characteristic for an RCM simulation and a scenario period) and a linear regression model for the dependence of changes ( $rts_m$ ) in rainfall (event/seasonal) characteristics on changes in  $RFO$  ( $T2M$ ) was fitted considering the whole RCM ensemble.

### PROJECTED CHANGES OF RAINFALL EVENT CHARACTERISTICS

Results related to changes in RCM-simulated rainfall (event/seasonal) mean characteristics, quantiles and histograms are described in this section. Relations between radiative forcing, temperature and rainfall event characteristics are summarized in at the end of this section.

#### Changes of mean rainfall (event/seasonal) characteristics

Mean characteristics of RCM-simulated heavy rainfall events for the control period (1981–2000) averaged over the study area are shown in the left part of Table 2. Relative changes of mean characteristics ( $rts_m$ ) for the RCM-simulated rainfall events between the control and the scenario periods for all grid boxes across the study area are shown as boxplots in Fig. 2.

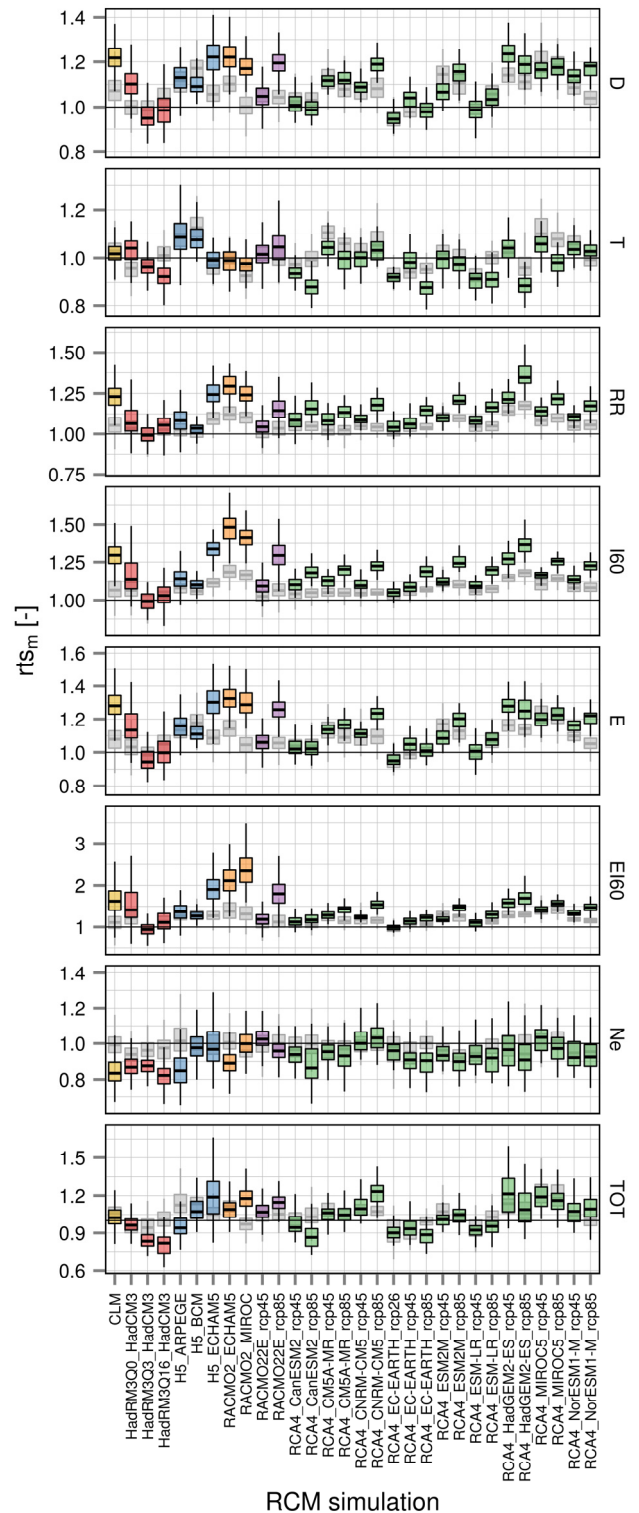


**Fig. 2.** Comparison of relative changes ( $rts_m$ ) in the RCM-simulated rainfall event characteristics for two scenario periods: 2020–2049 (SCE1, grey boxplots) and 2070–2099 (SCE2, coloured boxplots). Boxplots show relative changes in mean characteristics between the scenario periods and the control period for all grid boxes over the study area.

For the closer scenario period SCE1 the number of heavy events per season ( $Ne$ ) is approximately the same as for the control period for most RCM simulations.  $Ne$  is in general lower (by a maximum of two events per season) in the more distant scenario period SCE2. The changes in the seasonal total

**Table 2.** Mean heavy rainfall event characteristics (abbreviations are explained in section Methods) averaged over grid boxes in the Czech Republic in the control period (1981–2000) and their future changes in two scenario periods SCE1 (2020–2049) and SCE2 (2070–2099). Changes are evaluated as: insignificant changes below 5% (0); small changes between 5 and 10% (+); significant changes exceeding 10% (++); the largest significant changes exceeding 20% (+++); negative changes are denoted in the same way with sign (-).

| Acronym               | Control period |       |      |      |      |      |      |       |    |     |    | Changes in SCE1/SCE2 period |    |      |    |       |       |      |  |  |  |  |
|-----------------------|----------------|-------|------|------|------|------|------|-------|----|-----|----|-----------------------------|----|------|----|-------|-------|------|--|--|--|--|
|                       | Ne             | TOT   | D    | T    | RR   | I60  | E    | E/I60 | Ne | TOT | D  | T                           | RR | I60  | E  | E/I60 | Group |      |  |  |  |  |
| HadRM3Q3_HadCM3       | 10.51          | 209.0 | 19.5 | 21.6 | 1.04 | 3.01 | 2.01 | 8.56  | 0  | /-- | 0  | /0                          | 0  | /0   | 0  | /0    | -     | /0   |  |  |  |  |
| HadRM3Q16_HadCM3      | 10.31          | 231.7 | 21.6 | 23.2 | 1.11 | 3.48 | 2.27 | 11.8  | 0  | /-- | 0  | /-                          | 0  | /0   | 0  | /0    | ++    | /++  |  |  |  |  |
| RACMO22E_rep45        | 11.20          | 212.5 | 18.8 | 25.9 | 0.86 | 3.00 | 1.90 | 7.96  | 0  | /0  | +  | /0                          | 0  | /0   | +  | /+    | ++    | /++  |  |  |  |  |
| RCA4_EC-EARTH_rep26   | 11.11          | 249.7 | 21.7 | 26.4 | 0.95 | 2.44 | 2.11 | 5.86  | 0  | /-  | -  | /-                          | 0  | /+   | -  | /0    | 0     | /0   |  |  |  |  |
| RCA4_EC-EARTH_rep45   | 11.11          | 249.7 | 21.7 | 26.4 | 0.95 | 2.44 | 2.11 | 5.86  | -  | /-  | 0  | /0                          | 0  | /+   | 0  | /+    | +     | /++  |  |  |  |  |
| RCA4_ESM1-LR_rep45    | 11.45          | 257.9 | 21.9 | 25.0 | 1.06 | 2.72 | 2.17 | 6.65  | -  | /-  | 0  | /-                          | 0  | /+   | 0  | /0    | +     | /++  |  |  |  |  |
| CLM                   | 10.84          | 208.9 | 19.2 | 22.8 | 1.06 | 3.91 | 2.09 | 13.6  | 0  | /-- | +  | /0                          | +  | /+++ | +  | /+++  | ++    | /+++ |  |  |  |  |
| HadRM3Q0_HadCM3       | 11.33          | 278.3 | 23.9 | 23.2 | 1.28 | 4.20 | 2.62 | 16.9  | -  | /-- | 0  | /0                          | 0  | /+   | 0  | /++   | 0     | /+++ |  |  |  |  |
| HS_FCHAM5             | 11.11          | 224.7 | 19.0 | 20.5 | 1.13 | 2.91 | 1.92 | 6.54  | 0  | /0  | +  | /+++                        | +  | /+++ | +  | /+++  | ++    | /+++ |  |  |  |  |
| RACMO2_ECHAM5         | 9.42           | 191.0 | 20.2 | 26.6 | 0.91 | 2.81 | 2.02 | 7.69  | 0  | /-- | ++ | /+                          | ++ | /+++ | ++ | /+++  | ++    | /+++ |  |  |  |  |
| RACMO2_MIROC          | 9.67           | 217.8 | 22.4 | 31.1 | 0.85 | 2.74 | 2.24 | 8.63  | 0  | /0  | 0  | /+                          | ++ | /+++ | ++ | /+++  | ++    | /+++ |  |  |  |  |
| RACMO22E_rep85        | 11.20          | 212.5 | 18.8 | 25.9 | 0.86 | 3.00 | 1.90 | 7.96  | 0  | /0  | +  | /+                          | 0  | /++  | +  | /+++  | ++    | /+++ |  |  |  |  |
| RCA4_CM5A-MR_rep85    | 11.14          | 219.4 | 19.2 | 22.7 | 1.02 | 2.53 | 1.89 | 5.46  | 0  | /-  | 0  | /0                          | +  | /++  | +  | /++   | ++    | /+++ |  |  |  |  |
| RCA4_CNRM-CM5_rep45   | 12.38          | 289.2 | 22.5 | 25.0 | 1.07 | 2.77 | 2.23 | 6.94  | 0  | /0  | +  | /+                          | +  | /++  | +  | /++   | ++    | /+++ |  |  |  |  |
| RCA4_CNRM-CM5_rep85   | 12.38          | 289.2 | 22.5 | 25.0 | 1.07 | 2.77 | 2.23 | 6.94  | 0  | /0  | +  | /+                          | +  | /++  | +  | /++   | ++    | /+++ |  |  |  |  |
| RCA4_ESM2M_rep45      | 12.08          | 275.6 | 22.2 | 26.1 | 0.99 | 2.53 | 2.17 | 6.25  | 0  | /-  | +  | /0                          | ++ | /++  | ++ | /++   | ++    | /+++ |  |  |  |  |
| RCA4_ESM2M_rep85      | 12.08          | 275.6 | 22.2 | 26.1 | 0.99 | 2.53 | 2.17 | 6.25  | -  | /-  | 0  | /0                          | ++ | /+++ | ++ | /+++  | ++    | /+++ |  |  |  |  |
| RCA4_HadGEM2-ES_rep45 | 9.93           | 173.3 | 16.8 | 21.6 | 0.93 | 2.35 | 1.62 | 4.35  | 0  | /0  | ++ | /+++                        | ++ | /+++ | ++ | /+++  | ++    | /+++ |  |  |  |  |
| RCA4_MIROC5_rep85     | 10.11          | 221.2 | 21.2 | 23.0 | 1.11 | 2.83 | 2.11 | 6.67  | 0  | /0  | ++ | /+                          | ++ | /+++ | ++ | /+++  | ++    | /+++ |  |  |  |  |
| RCA4_NorESM1-M_rep45  | 11.76          | 233.8 | 19.2 | 21.9 | 1.03 | 2.57 | 1.89 | 5.41  | 0  | /0  | +  | /+                          | 0  | /++  | +  | /+++  | ++    | /+++ |  |  |  |  |
| RCA4_NorESM1-M_rep85  | 11.76          | 233.8 | 19.2 | 21.9 | 1.03 | 2.57 | 1.89 | 5.41  | 0  | /-  | 0  | /0                          | +  | /++  | +  | /+++  | ++    | /+++ |  |  |  |  |
| HS_ARPEGE             | 7.61           | 132.7 | 16.9 | 17.4 | 1.19 | 2.83 | 1.70 | 5.67  | 0  | /-- | ++ | /+                          | 0  | /+   | ++ | /+++  | ++    | /+++ |  |  |  |  |
| HS_BCM                | 12.70          | 246.6 | 18.5 | 20.5 | 1.08 | 2.51 | 1.83 | 5.27  | 0  | /0  | ++ | /+                          | ++ | /++  | ++ | /++   | ++    | /+++ |  |  |  |  |
| RCA4_CM5A-MR_rep45    | 11.14          | 219.4 | 19.2 | 22.7 | 1.02 | 2.53 | 1.89 | 5.46  | 0  | /0  | +  | /+                          | ++ | /++  | ++ | /++   | ++    | /+++ |  |  |  |  |
| RCA4_MIROC5_rep45     | 10.11          | 221.2 | 21.2 | 23.0 | 1.11 | 2.83 | 2.11 | 6.67  | 0  | /0  | ++ | /+                          | ++ | /++  | ++ | /+++  | ++    | /+++ |  |  |  |  |
| RCA4_CanESM2_rep45    | 10.65          | 221.5 | 20.0 | 23.9 | 1.01 | 2.63 | 1.97 | 6.01  | 0  | /0  | 0  | /-                          | +  | /++  | +  | /++   | +     | /++  |  |  |  |  |
| RCA4_CanESM2_rep85    | 10.65          | 221.5 | 20.0 | 23.9 | 1.01 | 2.63 | 1.97 | 6.01  | 0  | /-- | +  | /--                         | +  | /++  | 0  | /0    | +     | /++  |  |  |  |  |
| RCA4_EC-EARTH_rep85   | 11.11          | 249.7 | 21.7 | 26.4 | 0.95 | 2.44 | 2.11 | 5.86  | 0  | /-- | 0  | /--                         | 0  | /++  | 0  | /0    | +     | /+++ |  |  |  |  |
| RCA4_ESM1-LR_rep85    | 11.45          | 257.9 | 21.9 | 25.0 | 1.06 | 2.72 | 2.17 | 6.65  | 0  | /-  | 0  | /-                          | 0  | /++  | +  | /++   | ++    | /+++ |  |  |  |  |
| RCA4_HadGEM2-ES_rep85 | 9.93           | 173.3 | 16.8 | 21.6 | 0.93 | 2.35 | 1.62 | 4.35  | 0  | /-  | +  | /--                         | +  | /+++ | ++ | /+++  | ++    | /+++ |  |  |  |  |

due to heavy events ( $TOT$ ) are much more variable across the RCM simulations. While the simulated changes in  $TOT$  are larger than  $\pm 10\%$  only for 6 RCM simulations in the SCE1 period, in the SCE2 period the changes vary from a 20% decrease to a 19% increase (corresponding to a change ranging from  $-40$  to  $+54$  mm).

Four groups can be identified according to changes in grid box average rainfall event depth ( $D$ ), duration ( $T$ ), maximum 60-min intensity ( $I60$ ) and event rainfall energy ( $E$ ) as follows:

- RCM simulations with only small changes (below 10%) in all characteristics and scenario periods;
- RCM simulations with increasing  $D$ ,  $I60$ ,  $E$  and only small change (below 10%) in  $T$ ;
- RCM simulations with increasing  $D$ ,  $I60$ ,  $E$  and prevailing increase also in event duration ( $T$ );
- RCM simulations with increasing  $I60$  combined with decreasing  $T$ . The changes in  $D$  and  $E$  are small for most of these RCM simulations, except for RCA4\_HadGEM2-ES\_rcp85 with a significant increase in  $D$  and  $E$ .

A complete overview of changes of the considered event characteristics in the RCM simulations is given in Table 2.

### Quantile changes

Projected quantile changes ( $rt_{sp}$ ) between the control and two scenario periods are shown in Fig. 3. The changes are in general small ( $<10\%$ ) for most of the RCM simulations and quantiles in the SCE1 period, while there is a slight increase for the SCE2 period for all event characteristics except the event duration ( $T$ ), which is getting shorter.

In general, the increase is larger for larger values of  $D$ ,  $RR$ ,  $I60$ ,  $E$  and  $EI60$ , while the event duration ( $T$ ) remains on average the same for long events and decreases for the shortest heavy rainfall events.

### Histogram changes

Histogram changes ( $rt_{sp}$ ) between the control and scenario periods are similar for both scenario periods. In the SCE2 period (Fig. 4) the changes are slightly higher only for some characteristics. In general the number of heavy rainfall events with low  $D$ ,  $RR$ ,  $I60$ ,  $E$ ,  $EI60$  and high  $T$  is projected to decrease in most of the RCM simulations. The number of events with lowest depths ( $D < 13$  mm) and energies ( $E < 1$  MJ·ha $^{-1}$ ) clearly decreases, with the projected number of events in SCE2 being over 5 times smaller than that for the control period in several RCM simulations. Notable is also an increase in the number of rainfall events with moderate  $RR$  (2–4 mm·h $^{-1}$ ) and  $I60$  (4–10 mm·h $^{-1}$ ).

### Dependence on radiative forcing and projected temperature changes

For all emission (SRES A1B) and concentration (RCP) scenarios considered in this paper the estimated radiative forcing ( $RFO$ ) increases in the scenario periods. The increases are generally larger in the more distant (SCE2) period (exception is only the RCP2.6 scenario). The largest increases in the radiative forcing are estimated for the A1B and RCP8.5 scenarios in the SCE2 period as shown in Fig. 5. All RCM simulations indicate also increasing temperature ( $T2M$ ) with larger increases in the SCE2 period (on average  $\approx 3.2$  °C).

Most of the rainfall event characteristics in the ensemble of the RCM simulations depend on radiative forcing ( $RFO$ ) and temperature ( $T2M$ ) in a relatively similar way as demonstrated

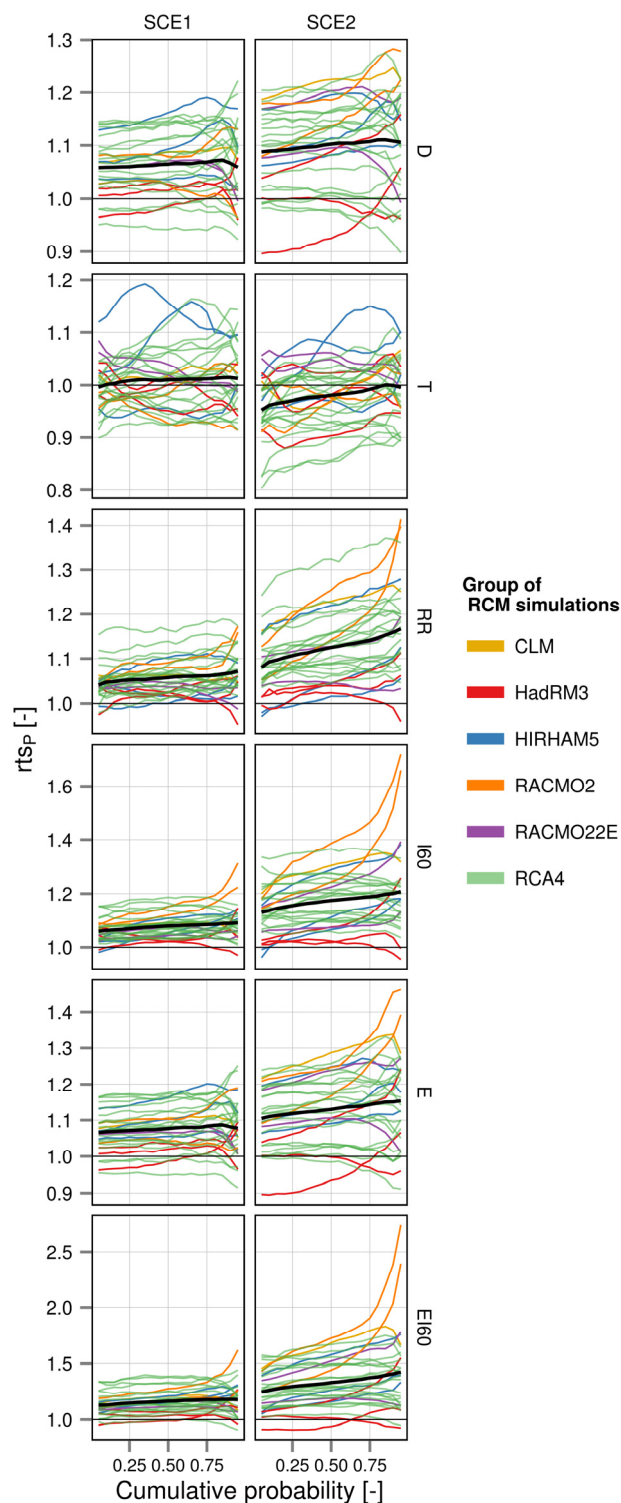


**Fig. 3.** Comparison of quantile changes ( $rt_{sp}$ ) in the RCM-simulated rainfall event characteristics for two scenario periods: 2020–2049 (SCE1) and 2070–2099 (SCE2). Thin lines represent the average from all grid boxes over the study area for each RCM simulation, bold black lines show ensemble average.

in Figs. 5 and 6. Slight differences occur for event depths ( $D$ ), which do not show any significant dependence on  $T2M$ , but slightly increase with  $RFO$  (statistically significant with  $p$ -value  $< 0.05$ ). On the other hand, event duration ( $T$ ) appears to be independent on  $RFO$ , but a decrease of  $T$  with increasing  $T2M$  is statistically significant ( $p$ -value  $< 0.01$ ). An increase in mean rainfall rate ( $RR$ ) and maximum 60-min rainfall intensity during

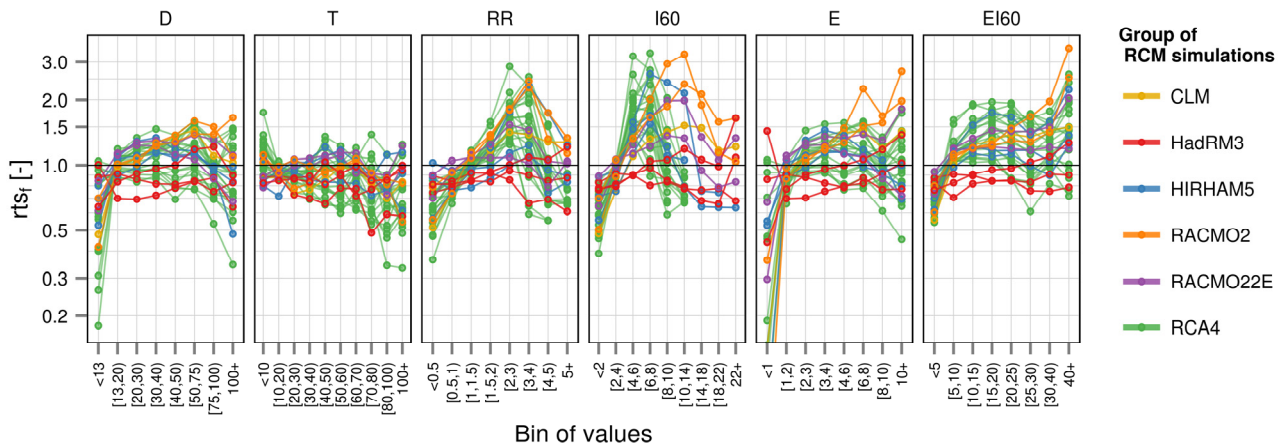


**Fig. 4.** Histogram changes ( $rts_f$ ) in the RCM-simulated rainfall event characteristics between the control period and scenario period SCE2 (2070–2099). Frequencies of bins in RCM simulations are averaged per one year and grid box over the study area.

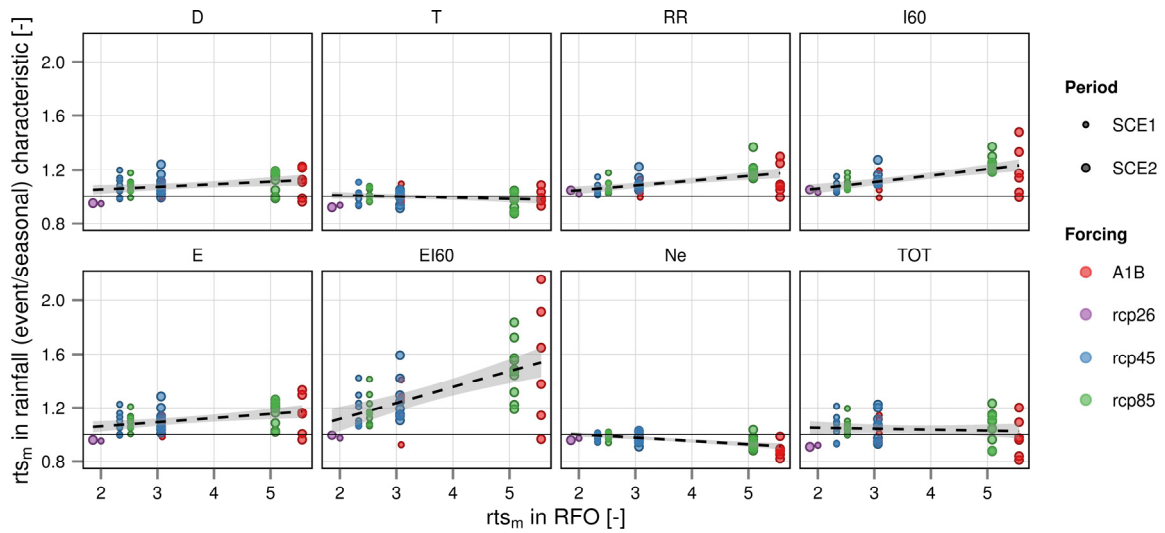


**Fig. 5.** Dependence of changes ( $rts_m$ ) in rainfall (event/seasonal) characteristics on changes ( $rts_m$ ) in radiative forcing ( $RFO$ ). All  $rts_m$  are averaged over the study area. The linear regression models fitted to the data (dashed lines) with the 95% confidence intervals (grey strips) are shown.

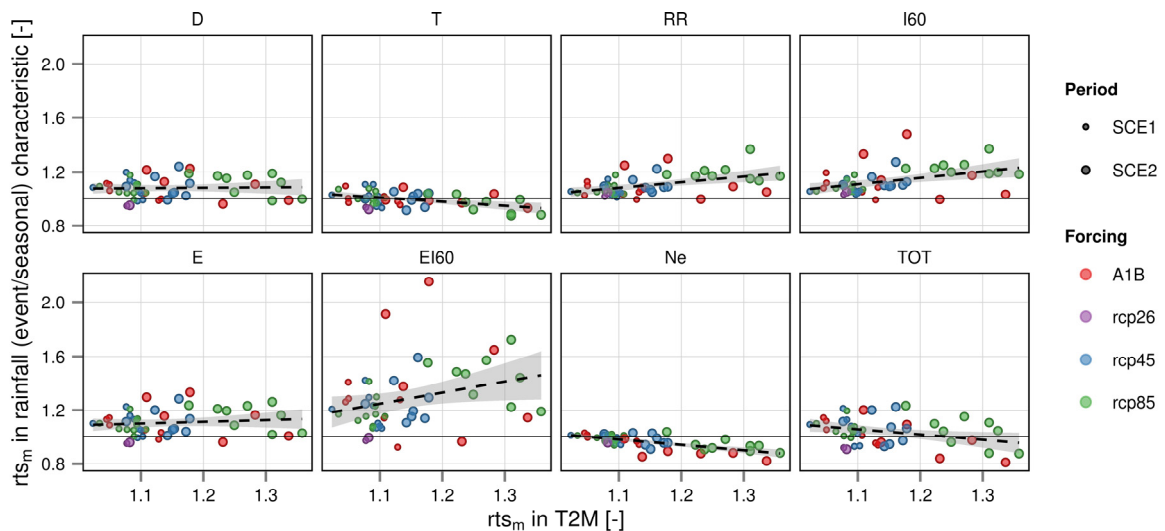


**Fig. 6.** Dependence of changes ( $rts_m$ ) in rainfall (event/seasonal) characteristics on changes ( $rts_m$ ) in temperature ( $T2M$ ). All  $rts_m$  are averaged over the study area. The linear regression models fitted to the data (dashed lines) with the 95% confidence intervals (grey strips) are shown.

an event ( $I60$ ) as well as a decrease in the number of heavy rainfall events per season ( $Ne$ ) are significant with increasing  $RFO$  and  $T2M$  ( $p$ -value  $< 0.01$ ). Ensemble averaged  $RR$  and  $I60$  increase at a rate of 6.5% and 9.1% per 1 °C, respectively.

Characteristics of extreme rainfall events (with non-exceedance probability  $p = 0.95$ ) in general show the same dependence on  $RFO$  and  $T2M$  as mean characteristics. Only  $RFO$  influence is slightly stronger compared to mean characteristics (slope coefficient  $\beta$  is only slightly larger; not shown).

## DISCUSSION

Projected changes in characteristics of heavy rainfall events in an ensemble of 30 RCM simulations were assessed for two scenario periods (2020–2049 and 2070–2099) against the control period (1981–2000). The RCM-simulated heavy rainfall events were identified considering 6-hour minimum inter-event time (MIT), 0.1 mm wet-hour threshold and top 15% rainfall events with the largest event depth for each RCM simulation.

Relative changes of the characteristics for RCM-simulated rainfall events are larger for the more distant scenario period (SCE2: 2070–2099). The number of heavy rainfall events is in general lower in the scenario periods (by a maximum of two events per season, i.e. 19%). Changes in the seasonal total due to heavy events vary from –20% to +19%.

According to the changes in mean characteristics of rainfall events for the scenario periods we identified 4 groups of RCM simulations. Large part of the RCM simulations (15 out of 30) were identified as simulations with increasing rainfall event depths ( $D$ ), maximum 60-min rainfall intensities ( $I60$ ), event rainfall energies ( $E$ ) and with relatively unchanged rainfall event durations ( $T$ ) through control and scenario periods. Considerable part of these RCM simulations shows larger than 20% increases in  $I60$  and  $E$  and at least 10% increase in event depths ( $D$ ) in the SCE2 period. As a consequence mean rainfall rate ( $RR$ ) and rainfall erosivity index ( $EI60$ ) increase as well. Six RCM simulations have only small changes in the considered characteristics (below 10%) and the 9 remaining RCM simulations project varied changes in event durations ( $T$ ) combined with increases in  $I60$  (4 with increasing  $T$  and 5 with decreasing  $T$ ). For comparison, Jacob et al. (2014) found statistically significant increases in total precipitation in large parts of Central Europe for the late 21<sup>st</sup> century from an ensemble of RCM simulations evaluated at the daily time scale (from the EURO-CORDEX and ENSEMBLES projects). For the Czech Republic, an increase in heavy summer precipitation up to 25% was reported. This increase was in general more pronounced in RCM simulations forced by RCP8.5 compared to SRES A1B and RCP4.5 scenarios (Jacob et al., 2014). From our analysis (which differs by considering the sub-daily time scale and individual rainfall events), changes in event depths ( $D$ ) as well as seasonal totals due to heavy rainfall events are smaller and in general not significantly different between the simulations forced by RCP8.5 and RCP4.5. However, the simulation with the highest spatial resolution RACMO22E (12.5 km) shows clearly larger increases in  $D$  for RCP8.5 when compared to RCP4.5. The situation is different for mean rainfall rates ( $RR$ ) and maximum 60-min rainfall intensities ( $I60$ ), since all RCM simulations forced by RCP8.5 yield larger increases compared to the RCP4.5 forced simulations.

The RCM simulations show slightly larger increases for larger (more extreme) values of rainfall event characteristics except for event duration ( $T$ ). The increases are most significant for the largest rainfall rates ( $RR$ ) and event rainfall erosivity

indices ( $EI60$ ). Shortest event durations ( $T$ ) slightly decrease in the SCE2 period. Although  $T$  is rather unchanged in the RCM simulations on average (and especially in the SCE1 period: 2020–2049), our findings are in general consistent with trends in erosive rainfall events found by Hanel et al. (2016) for the recent decades (increasing trends in rainfall rate and decreasing trends in event duration). Many other studies for western, northern and central Europe show increases in extreme precipitation intensities at daily (Frei et al., 2006; Hanel and Buishand, 2012; Hlavčová et al., 2015; Kyselý and Beranová, 2009; Kyselý et al., 2011) and sub-daily time scales (Arnbjerg-Nielsen, 2012; Hanel and Buishand, 2010). Jacob et al. (2014) concluded that at the daily scale, RCM simulations reduce weak precipitation intensities and project increases in moderate and high intensities for 2071–2100. This is consistent with an increase in  $RR$  and  $I60$  and a decrease in the number of heavy rainfall events with low  $RR$  and  $I60$  reported in our study. The intensification of hourly rainfall was also reported by Kendon et al. (2014) for the UK considering a convection-permitting model. On the other hand, the assessment of simulations at convection-permitting resolutions for Germany (Knote et al., 2010) and Western U.S. (Pan et al., 2011) revealed decrease in annual and summer hourly precipitation extremes, respectively.

Larger radiative forcing ( $RFO$ ) and increasing temperature ( $T2M$ ) in scenario periods (Houghton et al., 2001; Moss et al., 2010) are linked to characteristics of heavy rainfall events in the RCM simulations. The number of heavy rainfall events slightly decreases with larger  $RFO$  and  $T2M$ . While the effect is in general small for event depth ( $D$ ; increase with larger radiative forcing) and duration ( $T$ ; decrease with higher temperature), characteristics related to rainfall intensity show large significant increases with  $RFO$  and higher  $T2M$ . The estimated change in rainfall rate ( $RR$ ), i.e. 6.5% per °C corresponds well with the expectation from the Clausius-Clapeyron relation ( $\approx 7\%$ , see e.g. Lenderink and van Meijgaard, 2008). Although the increase in  $I60$  estimated in our study (9.1% per °C) is almost the same as that mentioned by Hanel and Buishand (2010) and also lies within the range reported by Lenderink and van Meijgaard (2008) for RCM-simulated data, much larger increases per °C were already reported for climate model simulations as well as for observed data, especially for convective rainfall events (e.g. Berg et al., 2013; Westra et al., 2014; Molnar et al., 2015). Note that in contrast to standard studies on precipitation-temperature scaling, where a fraction of largest (hourly) precipitation intensities is considered, here we analyse maximum hourly intensities within events selected on the basis of total event depth. This may lead to a situation when also less extreme  $I60$  are considered, which can partly explain relatively small increase in  $I60$  with temperature. In addition, given the dependence of the increase in  $I60$  on the exceedance probability (see Fig. 3) the scaling rate would be larger for more extreme  $I60$  than for the average  $I60$ . Finally, the increase may also be at least partly limited by available water vapour content.

Kendon et al. (2014) have shown that the changes derived from models allowing for convection might be considerably different than those from coarser resolution RCMs. Several other studies have also demonstrated a better skill of convection-permitting models in reproducing sub-daily precipitation characteristics, including the diurnal cycle and extremes (which are both closely linked to convection). Therefore, the projected changes in precipitation at short temporal scales from current RCMs have to be interpreted with caution.

The reported changes are averaged over the studied area. However, considerable spatial variability of changes can be

observed for each RCM simulation and characteristics. This spatial variability may be partly explained by altitude for changes in the number of heavy rainfall events (the decrease in the number of events is in general larger at high altitudes) and seasonal total due to heavy events (the decrease is larger or the increase is smaller at high altitudes).

## SUMMARY

The paper presents a contribution towards the currently limited knowledge on possible future changes in sub-daily precipitation extremes that are of great importance also for hydrological modelling and other applications. We analysed a large ensemble of 21<sup>st</sup> century RCM projections with a focus on heavy rainfall event characteristics. The main findings can be summarized as follows:

- For most of the RCM simulations the event depths (*D*), maximum 60-min rainfall intensities (*I60*) and event rainfall energies (*E*) are projected to increase, while the event durations (*T*) remain in general constant. More than one-third of all RCM simulations show increases exceeding 20% in *I60* and *E* and at least 10% in *D*.
- The changes are in general larger for larger values of rainfall event characteristics.
- Changes of rainfall event characteristics can to some extent be related to the changes in mean temperature and radiative forcing. Only changes in the number of heavy rainfall events and seasonal total due to heavy events depend significantly on altitude.
- The changes of calculated gradients of event rainfall rates (*RR*) per °C are generally consistent with the value expected from the Clausius-Clapeyron relation, except *I60* for which they are slightly larger.

The size of the analysed ensemble together with the focus on a wide range of event characteristics make our study rather unique in the context of climate change studies of sub-daily precipitation characteristics. Due to deficiencies in the convection parameterizations used in the current RCMs, however, the projected changes have to be interpreted with caution.

*Acknowledgements.* The research was supported by the Czech Science Foundation (project number 14-18675S) and the Ministry of the Interior of the Czech Republic (project number VG20122015092). We thank E. Buonomo (MOHC), O. B. Christensen (DMI), E. van Meijgaard (KNMI) and G. Nikulin (SMHI) for providing the sub-daily RCM data. We acknowledge the ENSEMBLES project, funded by the European Commission's 6th Framework Programme through contract GOCE-CT-2003-505539, and the World Climate Research Programme's Working Group on Regional Climate, and the Working Group on Coupled Modelling, former coordinating body of CORDEX and responsible panel for CMIP5. We also thank the climate modelling groups and institutions (listed in Table 1 of this paper) for producing and making available their model outputs.

## REFERENCES

Alexander, L.V., Zhang, X., Peterson, T.C., Caesar, J., Gleason, B., Klein Tank, A.M.G., Haylock, M., Collins, D., Trewin, B., Rahimzadeh, F., Tagipour, A., Rupa Kumar, K., Revadekar, J., Griffiths, G., Vincent, L., Stephenson, D.B., Burn, J., Aguilar, E., Brunet, M., Taylor, M., New, M., Zhai, P., Rusticucci, M., Vazquez-Aguirre, J.L., 2006. Global ob-

- served changes in daily climate extremes of temperature and precipitation. *J. Geophys. Res. Atmos.*, 111, D5. doi: 10.1029/2005JD006290.
- Arnbjerg-Nielsen, K., 2012. Quantification of climate change effects on extreme precipitation used for high resolution hydrologic design. *Urban Water J.*, 9, 2, 57–65. doi: 10.1080/1573062X.2011.630091.
- Beck, F., Bárdossy, A., Seidel, J., Müller, T., Sanchis, E.F., Hauser, A., 2015. Statistical analysis of sub-daily precipitation extremes in Singapore. *J. Hydrol.: Regional Studies*, 3, 337–358. doi: 10.1016/j.ejrh.2015.02.001.
- Berg, P., Haerter, J. O., 2013. Unexpected increase in precipitation intensity with temperature – a result of mixing of precipitation types? *Atmos. Res.*, 119, 56–61. doi: 10.1016/j.atmosres.2011.05.012.
- Berg, P., Moseley, C., Haerter, J. O., 2013. Strong increase in convective precipitation in response to higher temperatures. *Nat. Geosci.*, 6, 181–185. doi: 10.1038/NCEO1731.
- Blöschl, G., Nester, T., Komma, J., Parajka, J., Perdigão, R.A.P., 2013. The June 2013 flood in the Upper Danube Basin, and comparisons with the 2002, 1954 and 1899 floods. *Hydrol. Earth Syst. Sc.*, 17, 12, 5197–5212. doi: 10.5194/hess-17-5197-2013.
- Böhm, U., Kücken, M., Ahrens, W., Block, A., Hauffe, D., Keuler, K., Rockel, B., Will, A., 2006. CLM – the climate version of LM: brief description and long-term applications. *COSMO Newsl.*, 6, 225–235.
- Brockhaus, P., Lüthi, D., Schär, C., 2008. Aspects of the diurnal cycle in a regional climate model. *Meteorol. Z.*, 17, 4, 433–443. doi: 10.1127/0941-2948/2008/0316.
- Brown, L.C., Foster, G.R., 1987. Storm erosivity using idealized intensity distributions. *Trans. ASAE – Am. Soc. Agric. Eng.*, 30, 2, 379–386.
- Christensen, O.B., Drews, M., Christensen, J.H., Dethloff, K., Ketelsen, K., Hebestadt, I., Rinke, A., 2007. The HIRHAM regional climate model version 5 (beta). Technical Report, No. 06-17, Danish Climate Centre, Danish Meteorological Institute, Copenhagen, 22 p.
- Collins, M., Booth, B., Harris, G., Murphy, J., Sexton, D., Webb, M., 2006. Towards quantifying uncertainty in transient climate change. *Clim. Dynam.*, 27, 2–3, 127–147. doi: 10.1007/s00382-006-0121-0.
- Collins, M., Booth, B., Bhaskaran, B., Harris, G., Murphy, J., Sexton, D., Webb, M., 2011. Climate model errors, feedbacks and forcings: a comparison of perturbed physics and multi-model ensembles. *Clim. Dynam.*, 36, 9–10, 1737–1766. doi: 10.1007/s00382-010-0808-0.
- Dunkerley, D., 2008. Identifying individual rain events from pluviograph records: a review with analysis of data from an Australian dryland site. *Hydrol. Process.*, 22, 26, 5024–5036. doi: 10.1002/hyp.7122.
- Fiener, P., Neuhaus, P., Botschek, J., 2013. Long-term trends in rainfall erosivity – analysis of high resolution precipitation time series (1937–2007) from Western Germany. *Agr. Forest Meteorol.*, 171–172, 115–123. doi: 10.1016/j.agrformet.2012.11.011.
- Frei, C., Schöll, R., Fukutome, S., Schmidli, J., Vidale, P.L., 2006. Future change of precipitation extremes in Europe: intercomparison of scenarios from regional climate models. *J. Geophys. Res.*, 111, D6. doi: 10.1029/2005JD005965.
- Hand, W.H., Fox, N.I., Collier, C.G., 2004. A study of twentieth-century extreme rainfall events in the United Kingdom with implications for forecasting. *Meteorol. Appl.*, 11, 15–31. doi: 10.1017/S1350482703001117.
- Hanel, M., Buishand, T.A., 2010. On the value of hourly pre-

- precipitation extremes in regional climate model simulations. *J. Hydrol.*, 393, 3–4, 265–273. doi: 10.1016/j.jhydrol.2010.08.024.
- Hanel, M., Buishand, T.A., 2011. Analysis of precipitation extremes in an ensemble of transient regional climate model simulations for the Rhine basin. *Clim. Dynam.*, 36, 5–6, 1135–1153. doi: 10.1007/s00382-010-0822-2.
- Hanel, M., Buishand, T.A., 2012. Multi-model analysis of RCM simulated 1-day to 30-day seasonal precipitation extremes in the Czech Republic. *J. Hydrol.*, 412–413, 141–150. doi: 10.1016/j.jhydrol.2011.02.007.
- Hanel, M., Máca, P., 2014. Spatial variability and interdependence of rain event characteristics in the Czech Republic. *Hydrol. Process.*, 28, 6, 2929–2944, doi: 10.1002/hyp.9845.
- Hanel, M., Pavlásková, A., Kyselý, J., 2016. Trends in characteristics of sub-daily heavy precipitation and rainfall erosivity in the Czech Republic. *Int. J. Climatol.*, 36, 4, 1833–1845. doi: 10.1002/joc.4463.
- Hlavčová, K., Lapin, M., Valent, P., Szolgay, J., Kohnová, S., Rončák, P., 2015. Estimation of the impact of climate change-induced extreme precipitation events on floods. *Contributions to Geophysics and Geodesy*, 45, 3, 173–192. doi: 10.1515/congeo-2015-0019.
- Hohenegger, C., Brockhaus, P., Schär, C., 2008. Towards climate simulations at cloud-resolving scales. *Meteorol. Z.*, 17, 4, 383–394. doi: 10.1127/0941-2948/2008/0303.
- Houghton, J.T., Ding, Y., Griggs, D.J., Noguer, M., van der Linden, P.J., Dai, X., Makell, K., Johnson, C.A. (Eds.), 2001. *Climate change 2001: the scientific basis. Contribution of working group I to the third assessment report of the intergovernmental panel on climate change.* Cambridge University Press, Cambridge, UK and New York, USA, 94 p.
- Jacob, D., Petersen, J., Eggert, B., Alias, A., Christensen, O. B., Bouwer, L.M., Braun, A., Colette, A., Déqué, M., Georgievski, G., Georgopoulou, E., Gobiet, A., Menut, L., Nikulin, G., Haensler, A., Hempelmann, N., Jones, C., Keuler, K., Kovats, S., Kröner, N., Kotlarski, S., Kriegsmann, A., Martin, E., van Meijgaard, E., Moseley, C., Pfeifer, S., Preuschmann, S., Radermacher, C., Radtke, K., Rechid, D., Rounsevell, M., Samuelsson, P., Somot, S., Soussana, J.F., Teichmann, C., Valentini, R., Vautard, R., Weber, B., Yiou, P., 2014. EURO-CORDEX: new high-resolution climate change projections for European impact research. *Reg. Environ. Change*, 14, 2, 563–578. doi: 10.1007/s10113-013-0499-2.
- Jakob, D., Karoly, D.J., Seed, A., 2011. Non-stationarity in daily and sub-daily intense rainfall – part 1: Sydney, Australia. *Nat. Hazard. Earth Syst.*, 11, 8, 2263–2271. doi: 10.5194/nhess-11-2263-2011.
- Kendon, E.J., Roberts, N.M., Senior, C.A., Roberts, M.J., 2012. Realism of rainfall in a very high-resolution regional climate model. *J. Clim.*, 25, 17, 5791–5806, doi: 10.1175/JCLI-D-11-00562.1.
- Kendon, E.J., Roberts, N.M., Fowler, H.J., Roberts, M.J., Chan, S.C., Senior, C.A., 2014. Heavier summer downpours with climate change revealed by weather forecast resolution model. *Nat. Clim. Change*, 4, 7, 570–576. doi: 10.1038/nclimate2258.
- Kjellström, E., Boberg, F., Castro, M., Christensen, H.J., Nikulin, G., Sánchez, E., 2010. Daily and monthly temperature and precipitation statistics as performance indicators for regional climate models. *Clim. Res.*, 44, 2–3, 135–150. doi: 10.3354/cr00932.
- Knote, C., Heinemann, G., Rockel, B., 2010. Changes in weather extremes: assessment of return values using high resolution climate simulations at convection-resolving scale. *Meteorol. Z.*, 19, 1, 11–23. doi: 10.1127/0941-2948/2010/0424.
- Kundzewicz, Z.W. (Ed.), 2012. *Changes in Flood Risk in Europe.* IAHS Special Publication 10, CRC Press, Wallingford, UK, 544 p.
- Kundzewicz, Z.W., Ulbrich, U., Brücher, T., Graczyk, D., Krüger, A., Leckebusch, G.C., Menzel, L., Pińskwar, I., Radziejewski, M., Szwed, M., 2005. Summer floods in Central Europe – climate change track? *Nat. Hazards*, 36, 1–2, 165–189. doi: 10.1007/s11069-004-4547-6.
- Kupiainen, M., Samuelsson, P., Jones, C., Jansson, C., Willén, U., Hansson, U., Ullerstig, A., Wang, S., Döscher, R., 2011. Rossby Centre regional atmospheric model, RCA4. Rossby Centre Newsletter (June), SHMI, Norrköping, Sweden.
- Kyselý, J., 2009. Trends in heavy precipitation in the Czech Republic over 1961–2005. *Int. J. Climatol.*, 29, 12, 1745–1758. doi: 10.1002/joc.1784.
- Kyselý, J., Beranová, R., 2009. Climate-change effects on extreme precipitation in Central Europe: uncertainties of scenarios based on regional climate models. *Theor. Appl. Climatol.*, 95, 3–4, 361–374. doi: 10.1007/s00704-008-0014-8.
- Kyselý, J., Gaál, L., Beranová, R., Plavcová, E., 2011. Climate change scenarios of precipitation extremes in Central Europe from ENSEMBLES regional climate models. *Theor. Appl. Climatol.*, 104, 3–4, 529–542. doi: 10.1007/s00704-010-0362-z.
- Lautenschlager, M., Keuler, K., Wunram, C., Keup-Thiel, E., Schubert, M., Will, A., Rockel, B., Boehm, U., 2009a. Climate simulation with CLM, climate of the 20th century run no.2, data stream 3: European region MPI-M/MaD. World Data Center for Climate (WDCC), Max Planck Institute for Meteorology, Hamburg, Germany. doi: 10.1594/WDCC/CLM\_C20\_2\_D3.
- Lautenschlager, M., Keuler, K., Wunram, C., Keup-Thiel, E., Schubert, M., Will, A., Rockel, B., Boehm, U., 2009b. Climate simulation with CLM, scenario A1B run no.2, data stream 3: European region MPI-M/MaD. World Data Center for Climate (WDCC), Max Planck Institute for Meteorology, Hamburg, Germany. doi: 10.1594/WDCC/CLM\_A1B\_2\_D3.
- Lenderink, G., van Meijgaard, E., 2008. Increase in hourly precipitation extremes beyond expectations from temperature changes. *Nat. Geosci.*, 1, 8, 511–514. doi: 10.1038/ngeo262, 10.1038/ngeo262.
- Lenderink, G., Mok, H.Y., Lee, T.C., van Oldenborgh, G.J., 2011. Scaling and trends of hourly precipitation extremes in two different climate zones – Hong Kong and the Netherlands. *Hydrol. Earth Syst. Sci.*, 15, 9, 3033–3041. doi: 10.5194/hess-15-3033-2011.
- Madsen, H., Lawrence, D., Lang, M., Martinková, M., Kjeldsen, T., 2014. Review of trend analysis and climate change projections of extreme precipitation and floods in Europe. *J. Hydrol.*, 519, D, 3634–3650. doi: 10.1016/j.jhydrol.2014.11.003.
- Marchi, L., Borga, M., Preciso, E., Gaume, E., 2010. Characterisation of selected extreme flash floods in Europe and implications for flood risk management. Flash floods: observations and analysis of hydrometeorological controls, *J. Hydrol.*, 394, 1–2, 118–133. doi: 10.1016/j.jhydrol.2010.07.017.
- Meinshausen, M., Smith S.J., Calvin, K., Daniel, J.S., Kainuma, M.L., Lamarque, J.F., Matsumoto, K., Montzka, S.A., Raper, S.C., Riahi, K., Thomson, A., Velders, G.J., van

- Vuuren, D.P., 2011. The RCP greenhouse gas concentrations and their extensions from 1765 to 2300. *Clim. Change*, 109, 1–2, 213–241. doi: 10.1007/s10584-011-0156-z.
- Millán, M.M., 2014. Extreme hydrometeorological events and climate change predictions in Europe. *J. Hydrol.*, 518, Part B, 206–224. doi: 10.1016/j.jhydrol.2013.12.041.
- Molnar, P., Fatichi, S., Gaál, L., Szolgay, J., Burlando, P., 2015. Storm type effects on super Clausius–Clapeyron scaling of intense rainstorm properties with air temperature. *Hydrol. Earth Syst. Sci.*, 19, 1753–1766. doi: 10.5194/hess-19-1753-2015.
- Moss, R.H., Edmonds, J.A., Hibbard, K.A., Manning, M.R., Rose, S.K., van Vuuren, D.P., Carter, T.R., Emori, S., Kainuma, M., Kram, T., Meehl, G.A., Mitchell, J.F.B., Nakicenovic, N., Riahi, K., Smith, S.J., Stouffer, R.J., Thomson, A.M., Weyant, J.P., Wilbanks, T.J., 2010. The next generation of scenarios for climate change research and assessment. *Nature*, 463, 7282, 747–756. doi: 10.1038/nature08823.
- Nakicenovic, N., Swart, R. (Eds.), 2000. Special report on emissions scenarios: a special report of working group III of the Intergovernmental panel on climate change. Cambridge University Press, Cambridge, UK, 612 p.
- Pan, L.L., Chen, S.H., Cayan, D., Lin, M.Y., Hart, Q., Zhang, M.H., Liu, Y., Wang, J., 2011. Influences of climate change on California and Nevada regions revealed by a high-resolution dynamical downscaling study. *Clim. Dyn.*, 37, 9, 2005–2020. doi: 10.1007/s00382-010-0961-5.
- Rulfová, Z., Kyselý, J., 2013. Disaggregating convective and stratiform precipitation from station weather data. *Atmos. Res.*, 134, 100–115. doi: 10.1016/j.atmosres.2013.07.015.
- Rulfová, Z., Kyselý, J., 2014. Trends of convective and stratiform precipitation in the Czech Republic, 1982–2010. *Adv. Meteorol.*, Vol. 2014. doi: 10.1155/2014/647938.
- Samuelsson, P., Jones, C.G., Willén, U., Ullerstig, A., Gollvik, S., Hansson, U., Jansson, C., Kjellström, E., Nikulin, G., Wyser, K., 2011. The Rossby Centre regional climate model RCA3: model description and performance. *Tellus A*, 63, 1, 4–23. doi: 10.1111/j.1600-0870.2010.00478.x.
- Tolasz, R. (Ed.), 2007. Atlas podnebí Česka. [Climate atlas of Czechia]. 1st edn. Český hydrometeorologický ústav, Prague, Czech Republic, 255 p. (In Czech.)
- Trenberth, K.E., 2011. Changes in precipitation with climate change. *Clim. Res.*, 47, 1–2, 123–138. doi: 10.3354/cr00953.
- Utsumi, N., Seto, S., Kanae, S., Maeda, E.E., Oki, T., 2011. Does higher surface temperature intensify extreme precipitation? *Geophys. Res. Lett.*, 38, 16. doi: 10.1029/2011GL048426.
- van der Linden, P., Mitchell, J.F.B. (Eds.), 2009. ENSEMBLES: climate change and its impacts: summary of research and results from the ENSEMBLES project. Met. Office Hadley Centre, Exeter, UK, 160 p.
- van Meijgaard, E., van Ulft, L.H., van de Berg, W.J., Bosveld, F.C., van den Hurk, B., Lenderink, G., Siebesma, A.P., 2008. The KNMI regional atmospheric climate model RACMO version 2.1. Technical Report, TR 302, KNMI, De Bilt, Netherlands.
- van Meijgaard, E., van Ulft, L., Lenderink, G., de Roode, S., Wipfler, E., Boers, R., Timmermans, R., 2012. Refinement and Application of a Regional Atmospheric Model for Climate Scenario Calculations of Western Europe. KvR 054/12, Programme Office Climate changes Spatial Planning, KNMI, De Bilt, Netherlands, 47 p.
- van Vuuren, D., Edmonds, J., Kainuma, M., Riahi, K., Thomson, A., Hibbard, K., Hurtt, G., Kram, T., Krey, V., Lamarque, J.F., Masui, T., Meinshausen, M., Nakicenovic, N., Smith, S., Rose, S., 2011. The representative concentration pathways: an overview. *Clim. Change*, 109, 1–2, 5–31. doi: 10.1007/s10584-011-0148-z.
- Willems, P., Vrac, M., 2011. Statistical precipitation downscaling for small-scale hydrological impact investigations of climate change. *J. Hydrol.*, 402, 193–205. doi: 10.1016/j.jhydrol.2011.02.030.
- Wischmeier, W.H., Smith, D.D., 1978. Predicting rainfall erosion losses: a guide to conservation planning. *Agric. Handb.*, 537, Science and Education Administration, U.S. Department of Agriculture, Washington, D.C.
- Westra, S., Alexander, L.V., Zwiers, F.W., 2013. Global increasing trends in annual maximum daily precipitation. *J. Clim.*, 26, 11, 3904–3918. doi: 10.1175/JCLI-D-12-00502.1.
- Westra, S., Fowler, H.J., Evans, J.P., Alexander, L.V., Berg, P., Johnson, F., Kendon, E.J., Lenderink, G., Roberts, N.M., 2014. Future changes to the intensity and frequency of short-duration extreme rainfall. *Rev. Geophys.*, 52, 3, 522–555. doi: 10.1002/2014RG000464.

Received 21 December 2015

Accepted 25 May 2016